

Matched regulation of gastrointestinal performance in the Burmese python, *Python molurus*

Christian L. Cox* and Stephen M. Secor

Department of Biological Sciences, The University of Alabama, Tuscaloosa, AL 35487-0344, USA

*Author for correspondence at present address: Department of Biology, The University of Texas at Arlington, Arlington, TX 76019-0498, USA
 (e-mail: clcox@uta.edu)

Accepted 4 February 2008

SUMMARY

In Burmese pythons fasting and feeding cause dramatic regulation of gastric acid production and intestinal nutrient uptake. Predictably, other components of their gastrointestinal tract are similarly regulated with each meal. We therefore assessed the matched regulation of gastrointestinal performance by comparing the postprandial activities and capacities of gastric (pepsin), pancreatic (amylase and trypsin) and intestinal (aminopeptidase-N and maltase) enzymes, and intestinal nutrient uptake. Tissue samples were collected from pythons fasted and at 0.25, 0.5, 1, 2, 3, 4, 6, 10 and 15 days following their consumption of rodent meals equaling 25% of snake body mass. With feeding, pythons experience no significant change in stomach mass, whereas both the pancreas and small intestine doubled in mass. Feeding also triggered a depletion of gastric mucosal pepsinogen, a respective 5.7- and 20-fold increase in the peak activities of pancreatic trypsin and amylase, and a respective 2.3- and 5.5-fold increase in the peak activities of intestinal maltase and aminopeptidase-N. Enzyme activities peaked between 2 and 4 days postfeeding and returned to fasting levels by day 10. Independent of digestive stage, python intestine exhibited a proximal to distal decline in enzyme activity. For both sugars and proteins, intestinal capacities for enzyme activity were significantly correlated with nutrient uptake capacities. The concomitant postprandial upregulation of tissue morphology, intestinal nutrient transport rates and enzyme activities illustrate, for the python, the matched regulation of their gastrointestinal performance with each meal.

Key words: correlated response, digestion, digestive enzyme, intestinal nutrient, transport, python, reptile.

INTRODUCTION

Theoretically, the components of a physiological system (e.g. respiratory, cardiovascular or renal) are matched in functional capacity (maximal ability of a tissue) such that energy and space are not wasted because of an unbalanced design of the limits of tissue performance (Weibel et al., 1991; Diamond, 2002). This concept, coined ‘symmorphosis’, predicts that both structure and function are coordinated to the actual demand on the system, because any departure from the matching of functional capacities will be manifested in a decreased efficiency of performance and energy flux, resulting in a reduction in fitness (Weibel et al., 1991). Moreover, changes in demand are often met by phenotypic remodeling of tissue morphology and capacity, such as hypertrophy of muscles with exercise, increase in the red blood cells and lung capacity in response to hypoxia, and atrophy and hypertrophy of the digestive tract in response to fasting and refeeding (McDonagh and Davies, 1984; Secor and Diamond, 1995; Haldol et al., 2004; Beall, 2006). The match between tissue performance and demand has been studied for the mammalian pulmonary system (Taylor et al., 1996), the renal system of desert mammals (Lindstedt and Jones, 1988), enzyme expression in human erythrocytes (Salvador and Savageau, 2003) and glycolytic enzymes in tuna muscles (Fudge et al., 2001). Symmorphosis is not without controversy, however, as both the logical underpinning and the evidence supporting this hypothesis have been challenged (Garland and Huey, 1987; Dudley and Gans, 1991).

The gastrointestinal (GI) tract is an equally amenable system to study matched responses to changes in demand. This system

includes a variety of different organs and tissues that operate in a coordinated, sequential fashion to break down and absorb ingested nutrients. The serial match between load and functional capacity in digestion has been documented for intestinal enzyme activity and nutrient transport in mice (O’Connor and Diamond, 1999; Lam et al., 2002). Also well established is the plasticity of the digestive tract to changes in demand (Piersma and Lindström, 1997), observed as morphological and functional responses to events such as lactation (Hammond and Diamond, 1994), changes in diet (Weiss et al., 1998), migration (McWilliams and Karasov, 2001), fasting (Secor and Diamond, 1995; Haldol et al., 2004), estivation (Cramp and Franklin, 2005) and hibernation (Carey, 1990). Given the phenotypic plasticity of the gut, studying how the various components of the GI tract respond to a change in load would provide insight into the proposed adaptive matching of functional capacities for a physiological system.

To experimentally explore the matching of GI performance, we used the Burmese python (*Python molurus*), which has been shown in a number of recent studies to be a suitable model for the investigation of physiological responses to fasting and digestion (Secor and Diamond, 1998; Overgaard et al., 1999; Lignot et al., 2005). This python experiences rapid (within 24 h of consuming a meal) and dramatic postprandial increases in metabolism (Secor and Diamond, 1997; Overgaard et al., 2002), release of GI hormones (Secor et al., 2001), cardiac performance (Secor et al., 2000a), gastric function (Secor, 2003) and intestinal nutrient transport (Secor and Diamond, 1995). Concurrent morphological changes include 30–100% increase in heart, liver, pancreatic, kidney and small

intestinal mass, and a fourfold lengthening of intestinal microvilli (Secor and Diamond, 1995; Lignot et al., 2005). Moreover, after completing digestion, the Burmese python downregulates the aforementioned postfeeding responses to fasting levels within 10–14 days after feeding. The large regulatory response of the Burmese python is proposed to be an adaptation to predictable, long periods of fasting, allowing energy to be conserved during the extended bouts of digestive quiescence (Secor and Diamond, 2000).

Beyond temporal variation, the small intestine of the Burmese python exhibits a spatial gradient of both structure and function from the proximal to distal end, with the proximal small intestine weighing more, possessing longer villi, and greater rates of nutrient transport activity than the distal small intestine (Secor and Diamond, 1995; Lignot et al., 2005). Combining the python's wide regulation of gastric (e.g. acid production) and intestinal (e.g. nutrient uptake) function and the theoretical consideration that regulatory responses are matched in magnitude, we hypothesize that the Burmese python experiences similar temporal and spatial patterns in the activity of digestive enzymes in response to feeding and fasting, and that the regulation of gastric, pancreatic and intestinal performance for the python is closely coupled in time and magnitude.

To explore these hypotheses, we analyzed: (1) the temporal variation in the activities of gastric, pancreatic and small intestinal enzymes; (2) the spatial variation along the length of the small intestine in enzyme activities; and (3) the temporal match in the regulation of GI capacities for enzyme activities and intestinal nutrient uptake. To evaluate the potential integrative regulation of gastrointestinal performance, we measured, from fasted and fed animals (0.25–15 days postfeeding), the activities of gastric pepsin, pancreatic trypsin and amylase, and small intestinal aminopeptidase-N and maltase, as well as capacities of intestinal L-leucine, L-proline and D-glucose brushborder transport. In this study, we demonstrate that the Burmese python exhibits postprandial variation in digestive morphology, enzyme activity and nutrient uptake, spatial variation of intestinal function and morphology, and matched regulation of gastric, pancreatic and intestinal performance.

MATERIALS AND METHODS

Snake maintenance and tissue collection

Hatchling pythons (*Python molurus* L.) were purchased commercially (Bob Clark Captive Bred Reptiles, Oklahoma City, OK, USA; Strictly Reptiles Inc., Hollywood, FL, USA) and housed individually in 20 l plastic containers placed within customized racks (Animal Plastics, Johnston, IA, USA). A heat cable fitted into the back of each rack provided a front to back temperature gradient of 28–32°C. Snakes were maintained under a photoperiod of 14 h:10 h L:D, fed laboratory rats once every 2 weeks, and had continuous access to water. Experiments were performed on pythons maintained at 30°C either after a 30 day fast or at 0.25, 0.5, 1, 2, 3, 4, 6, 10, or 15 days following the consumption of a single rat meal weighing $25.00 \pm 0.02\%$ of snake body mass (four snakes per sampling period). To reduce potential body-size effects, snakes were selected for each time point such that there were no significant (all $P > 0.9$) differences in body mass (838 ± 9 g), snout–vent length (126 ± 1 cm) or total length (142 ± 1 cm) among sampled time points. Pythons were killed by severing the spinal cord immediately posterior to the head and a mid-ventral incision was made to expose the internal organs for removal and processing as described below. Animal care and experimentation were conducted under protocols approved by the University of Alabama Institutional Animal Care and Use Committee.

Tissue mass

After removal from the snake, the stomach, pancreas and small intestine were weighed, emptied of any contents (stomach and small intestine) and reweighed. The difference in mass between the full and emptied stomach and small intestine provided an estimate (assuming an addition to content mass from secretions) of the remaining mass of the meal within each organ. Segments of the pancreas and stomach were snap frozen in liquid N₂ and much of the remaining portion was dried to a constant mass at 60°C to calculate total organ dry mass. The emptied small intestine was divided into five equal-length segments, designated A (most proximal), B, C, D and E (most distal). Each segment was weighed, everted, and for a 2 cm portion, the mucosa was scraped from the underlying muscularis/serosa layer and snap frozen in liquid N₂. In addition, we scraped the mucosa from a 1 cm portion of each segment and weighed separately the scraped mucosa and remaining muscularis/serosa.

Gastric pepsin assay

The activity of the peptidase pepsin (E.C. 3.4.23.1) from the stomach mucosa was measured following the procedure of Anson (Anson, 1938). Scraped mucosa from the mid-region of the stomach was homogenized in PBS buffer (pH 6.9, 1:10 dilutions) on ice, centrifuged for 20 min at 3300 g (at 4°C), and the supernatant diluted five times with buffer. Activity of pepsin was measured using 0.031 mmol l⁻¹ hemoglobin (pH 2.0, using 300 mmol l⁻¹ HCl, 37°C), which when cleaved by pepsin leaves tyrosine residues that absorb light at 280 nm. The reaction was terminated after 30 min with 5% trichloroacetic acid. Absorbance of samples were measured spectrophotometrically (DU 530, Beckman Coulter, Inc., Fullerton, CA, USA) at 280 nm and compared to a L-tyrosine standard curve. For this and other enzyme assays, enzyme activities were quantified as μmol of substrate liberated per minute of incubation per gram of protein. Protein content of all homogenates was determined using a Bio-Rad Protein Assay kit based on the method of Bradford (Bradford, 1976).

Pancreatic amylase assay

We calculated the activity of pancreatic amylase (EC 3.2.1.1) following the procedure of Bernfeld (Bernfeld, 1955). Pancreas segments were homogenized in PBS buffer (pH 6.9, 1:10 dilution) on ice, centrifuged for 20 min at 30 000 g (at 4°C), and the supernatant further diluted 100 \times with buffer. Diluted supernatant was incubated with 1% amylose for 3 min at 37°C. The reaction was terminated with Sumner reagent (0.5 mol l⁻¹ NaOH, 28.8 mol l⁻¹ dinitrosalicylic acid and 0.9 mol l⁻¹ sodium potassium tartarate). Amylase activity was quantified by comparing the absorbance of the sample at 540 nm to a glucose standard curve.

Pancreatic trypsin assay

Pancreatic trypsin activity (EC 3.4.21.4) was quantified following the procedure of Preiser et al. (Preiser et al., 1975). Because trypsin is secreted from the pancreas as an inactive zymogen, we also measured trypsin activity in small intestine contents of pythons between 12 h and 6 days after feeding. Pancreas segments or small intestinal contents were homogenized in PBS buffer (pH 6.9, 1:10 dilution) on ice, centrifuged for 20 min at 30 000 g (at 4°C), and the supernatant was diluted a further 200 \times with buffer. Following trypsinogen activation by a 1% enterokinase solution, trypsin activity was measured using 0.91 mmol l⁻¹ N- α -benzoyl-L-arginine p-nitroanilide hydrochloride as the substrate (0.91 mmol l⁻¹, 37°C), which trypsin cleaves to form p-nitroanilide. The reaction was

terminated after 30 min with 30% acetic acid. Trypsin activity was determined from the absorbance of the sample, measured spectrophotometrically at 410 nm and compared to a p-nitroanilide standard curve.

Intestinal aminopeptidase-N

We measured, from each segment of the small intestine, the activity of the brush border-bound hydrolase, aminopeptidase-N (APN; EC 3.4.11.2) following the procedure of Wojnarowska and Gray (Wojnarowska and Gray, 1975). Scraped intestinal mucosa was homogenized in PBS buffer (pH 7.0, 1:250 dilution) on ice and the activity of aminopeptidase-N in the homogenate was measured following incubation with 0.34 mmol l⁻¹ leucyl-β-naphthylamide (LNA) as the substrate (30 min) and p-hydroxymercuribenzoic acid to inhibit nonspecific cytosol peptidases. The reaction was terminated after 30 min with 40% trichloroacetic acid. Absorbance of the β-naphthylamide resulting from the hydrolysis of LNA was measured spectrophotometrically at 560 nm and compared to a standard curve developed with β-naphthylamine.

Intestinal maltase assay

From each segment of the small intestine, we measured the activity of the brush border-bound disaccharidase, maltase (EC 3.2.1.20) following the procedure of Dahlqvist (Dahlqvist, 1984). We homogenized scraped mucosa in buffer (pH 7.0, 23 mmol l⁻¹ PBS, 5 mmol l⁻¹ Tris-HCl, 1 mmol l⁻¹ EDTA, 0.17 mmol l⁻¹ Triton X-100; 1:10 dilution), added to a PBS buffer to prevent inhibition of maltase by Tris (pH 7.0, 1:5 dilution). The diluted sample was incubated in 62.5 mmol l⁻¹ maltose (37°C), and maltase activity calculated from the amount of glucose liberated as indicated by the addition of Glucostat solution (250 mmol l⁻¹ Tris buffer, 0.002 mg ml⁻¹ horseradish peroxidase, 10 mmol l⁻¹ p-hydroxybenzoic acid, 0.2 mmol l⁻¹ aminoantipyrine, and 0.0334 mg ml⁻¹ glucose oxidase), which also terminated the reaction at 30 min. Absorbance of the end product was measured spectrophotometrically at 500 nm and compared to a glucose standard curve for Glucostat.

Intestinal enzyme capacity

We quantified the capacity for each enzyme as the product of tissue mass and mass-specific rates of enzyme activity (μmol min⁻¹ g⁻¹ tissue). For the pancreas we used the wet mass of the intact pancreas, whereas for the stomach and the five segments of the small intestine we use the relative wet mass of the scraped mucosa to calculate the total organ mucosal mass.

Intestinal nutrient uptake capacity

We calculated intestinal uptake capacity for amino acids L-leucine and L-proline, and the sugar D-glucose by summing the product of segment mass (mg) and segment mass-specific rates of nutrient uptake (nmol min⁻¹ mg⁻¹) for the five intestinal segments. Rates of nutrient uptake across the intestinal brush border membrane were measured using the everted sleeve technique (Karasov and Diamond, 1983; Secor et al., 1994). Sleeves of the everted intestine (1 cm long) were preincubated for 5 min in reptile Ringer's solution (30°C), and then incubated for 2 min in reptile Ringer's solution containing both an unlabeled and radiolabeled nutrient (³H-L-leucine, ³H-L-proline or ¹⁴C-D-glucose) and a radiolabeled adherent fluid marker (¹⁴C-polyethylene glycol for amino acids or ³H-L-glucose for D-glucose). We measured, from each intestinal segment, the total uptake (passive and carrier-mediated) of each amino acid and the carrier-mediated uptake of D-glucose (nmol min⁻¹ mg⁻¹).

Statistical methods

We used one-way and repeated-measures ANOVA to test for significant differences in enzyme activity among time points and among intestinal segments, respectively. We tested for significant differences in organ and tissue masses and capacities of enzyme activity and nutrient uptake using one-way ANCOVA, with body mass as the covariate. Each ANOVA and ANCOVA resulting in a significant difference was followed by a pairwise mean comparison (Tukey-Kramer procedure) to test for differences between time points and position. We evaluated the relationships among organ capacities by (1) qualitatively assessing the matched regulation of the components and capacities of the digestive tract and (2) using a statistical approach (Pearson product moment correlation procedure) to quantify the coordination among capacities. We designate the level of significance as $P < 0.05$ and report mean values as means ± 1 s.e.m.

RESULTS

Tissue mass

We found no significant (all $P > 0.15$) variation among sampling times in the wet or dry mass of the intact stomach or in the wet mass of its mucosa or serosa components (Fig. 1). By contrast, wet and dry mass of the pancreas varied significantly (both $P < 0.001$)

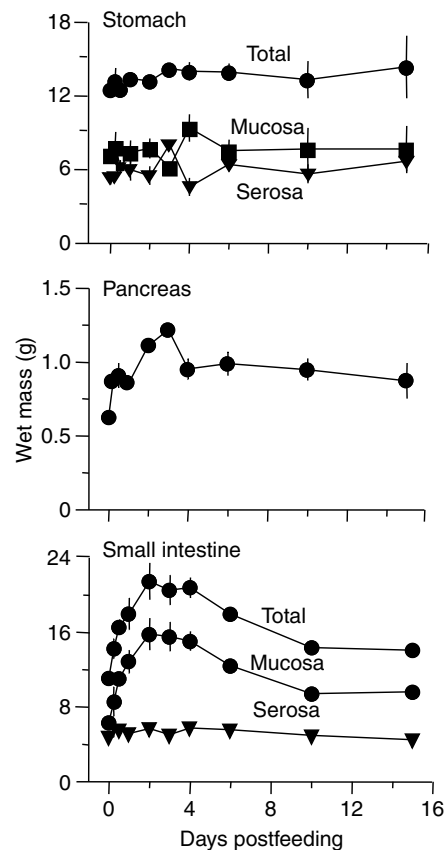


Fig. 1. Total, mucosal and serosal wet mass of the stomach and small intestine, and pancreas wet mass of *Python molurus* as a function of days postfeeding. Note the postprandial increase in the mass of the pancreas and small intestine, and the lack of change in stomach and intestinal serosal mass. In this and similar figures, error bars indicate ± 1 s.e.m. and are omitted if the s.e.m. is smaller than the width of the symbol used for the mean value.

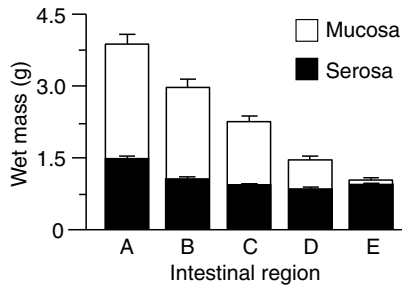


Fig. 2. Mucosal, serosal and total wet mass averaged over all time points for five intestinal segments of *Python molurus*, with segment A the most proximal and E the most distal. Note the gradual decline in tissue mass from the proximal to distal ends of the small intestine.

among fasted and fed pythons (Fig. 1). By day 2 of digestion, the pancreas had doubled in wet mass, and remained significantly heavier until day 10. Likewise, the small intestine varied significantly ($P < 0.001$) in mass among time points, increasing as much as 92% by 2 days postfeeding (Fig. 1). In similar fashion each of the five segments of the small intestine varied significantly (all $P < 0.001$) in mass among sampling periods. For each segment we found mucosal wet mass to vary significantly (all $P < 0.005$) among sampling periods, whereas the wet mass of muscularis/serosa did not change as a function of sampling time. Independent of the temporal changes, segment mucosal, serosal and total mass also varied significantly (all $P < 0.001$) spatially (Fig. 2). The mucosal, serosal and total mass of the most proximal segment (A), averaged 140%, 70% and 180% heavier, respectively, than for the most distal segment (E).

Gastric performance

The percentage of original meal mass remaining in the stomach declined over time such that by day 6 of digestion only $3.4 \pm 1.5\%$ of the meal remained in the stomach (Fig. 3). Gastric evacuation rate, quantified as the difference between an individual stomach contents and the mean stomach contents of the immediately previous sampling period divided by the time elapsed between those sampling times, varied significantly ($P < 0.001$) among sampling times, and was greatest for pythons between 12 and 24 h after feeding (Fig. 3), during which time $17.9 \pm 3.8\%$ of the meal passed into the small intestine. Pepsin activity measured in the gastric mucosa varied significantly ($P = 0.03$) among sampling periods, with highest pepsin activity in fasted animals and animals 6, 10, and 15 days postfeeding (Fig. 4). Pepsin capacity (the product of stomach mucosa mass times pepsin activity) varied significantly ($P = 0.04$), and followed a similar pattern to pepsin activity (Fig. 4).

Pancreatic enzymes

Pancreatic trypsin activity varied significantly ($P < 0.001$) among sampling periods, increasing ($P = 0.03$) by 6 h after feeding before peaking at 5.7-fold that of fasted levels by day 4 of digestion (Fig. 5). Trypsin activity of proximal small intestinal contents increased significantly ($P < 0.001$) by day 3, to threefold the activity of snakes 12 h after feeding, and returned to fasted activity by day 6 (Fig. 5). Pancreatic amylase activity also varied significantly ($P < 0.001$) among sampling periods, increasing within 2 days after feeding, peaking at 20-fold of fasted levels by day 4 of digestion, and returning to fasted activities by day 10 (Fig. 5). Pancreatic trypsin and amylase capacity (the product of pancreas wet mass and enzyme activity) also varied significantly (both $P < 0.001$) among sampling

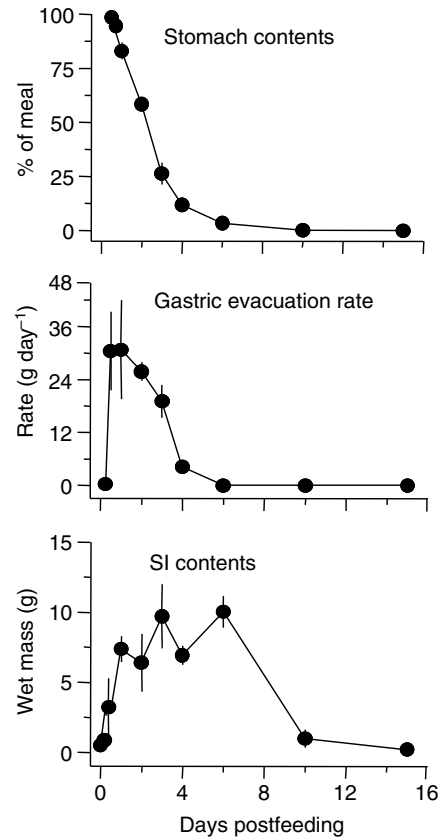


Fig. 3. Stomach contents (% of meal mass), gastric evacuation rate and small intestine (SI) contents (in g) as a function of days postfeeding for *Python molurus*. Gastric evacuation rate is defined as the difference between individual stomach contents and the mean stomach contents of the immediately previous sampling period divided by the time elapsed between those sampling times. Note between 12 h and 3 days postfeeding that much of the ingested meal passes from the stomach into the small intestine.

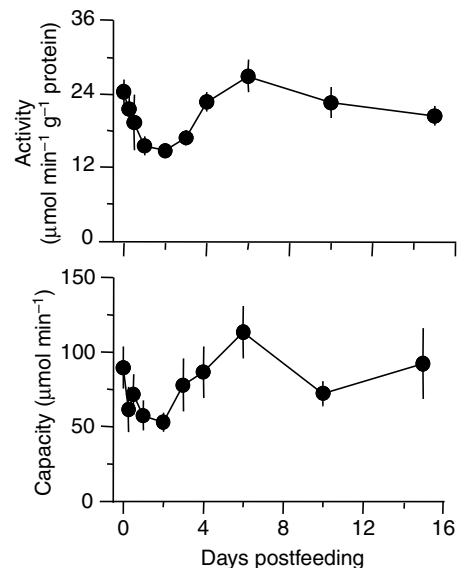


Fig. 4. Gastric mucosal pepsin activity and capacity as a function of days postfeeding for *Python molurus*. Note the rapid postprandial decline in mucosal pepsin, indicating the release of the precursor pepsinogen which is converted to the proteolytic pepsin.

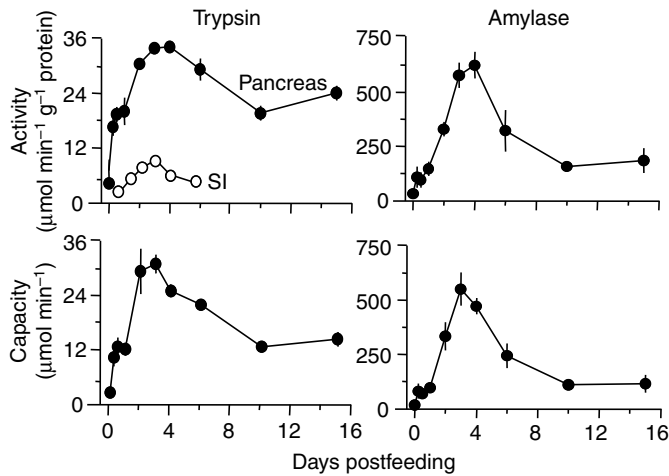


Fig. 5. Pancreatic trypsin and amylase activity (top panel) and capacity (bottom panel) as a function of days postfeeding for *Python molurus*. Trypsin activity of the intestinal luminal fluid (0.5–6 days after feeding) is also presented in the top left panel. Both pancreatic enzymes experience a rapid upregulation in capacity after feeding.

periods (Fig. 5). Trypsin and amylase capacity peaked at 3 days postfeeding at 12- and 35-fold of fasting capacities, respectively, before returning to fasting levels by day 10.

Small intestinal performance

Small intestinal contents varied significantly ($P < 0.001$) in mass among sampling periods, averaging 8.1 ± 1.4 g between 1 and 6 days postfeeding (Fig. 3). For the five intestinal segments, APN activity varied significantly (all $P < 0.007$) among each of the time points, having increased (all $P < 0.05$) within 24 h after feeding. Peaks in APN activity occurred at day 1 (segment E) or day 3 (segments A, B, C and D) following a 4.2- to 5.5-fold increase over fasted levels (Fig. 6). Although there was a general trend of a decrease in APN activity from the proximal to the distal ends of the small intestine, the difference was only statistically significant (both $P < 0.05$) at 0.25

and 6 days postfeeding. On average, APN activity of the first four segments was $52 \pm 4\%$ greater than that of the last segment (Fig. 7). The calculated summed capacity for APN activity varied significantly ($P < 0.01$) among sampling periods, increasing to 7.9-fold fasted capacity by day 1, peaking at 12.3-fold of fasted capacity by day 3 and returning to fasted levels by day 10 (Fig. 8).

We found only the most proximal segment (A) to experience significant ($P = 0.009$) postfeeding regulation in maltase activity. By day 2 of digestion, maltase activity of the first segment had increased by 130% before returning to prefeeding levels by day 4. For the python small intestine, there is an observable positional gradient in maltase activity during digestion as activity declines distally (Fig. 6). When averaged for all 10 sampling periods, maltase activity of segments A, B, C and D were 170%, 110%, 90%, 60% greater, respectively, than the activity of segment E. We found total intestinal maltase capacity to vary significantly ($P = 0.007$) among sampling periods, with a 3.3-fold increase by day 3, and returning to fasting levels by day 6 of digestion (Fig. 8).

Intestinal uptake capacity of each nutrient was significantly (all $P < 0.001$) upregulated within 12 h after feeding (Fig. 9). Capacities peaked at 2 days postfeeding at 5.7, 6.2 and 12.8-fold of fasting levels for L-leucine, L-proline and D-glucose, respectively (Fig. 9). Uptake capacities of each nutrient remained significantly elevated before returning to fasted levels by day 10.

Integrated response

The python's postprandial match in the regulation of gastrointestinal performance is suggestive of an integrated response. For both pathways of protein and carbohydrate digestion and absorption, tissue enzyme and transporter capacities peaked at 2 and 3 days postfeeding (Fig. 10). For protein digestion and absorption, we found that trypsin, APN and both L-leucine and L-proline uptake capacity were significantly (all $P < 0.0001$, $r^2 = 0.64-0.81$) correlated with each other. Likewise, for carbohydrate digestion and absorption, amylase, maltase, and D-glucose uptake capacity were significantly (all $P < 0.006$, $r^2 = 0.43-0.60$) correlated with each other. The exception to the above was the postprandial decline in gastric mucosal pepsin activity as the precursor pepsinogen was released to increase luminal pepsin content.

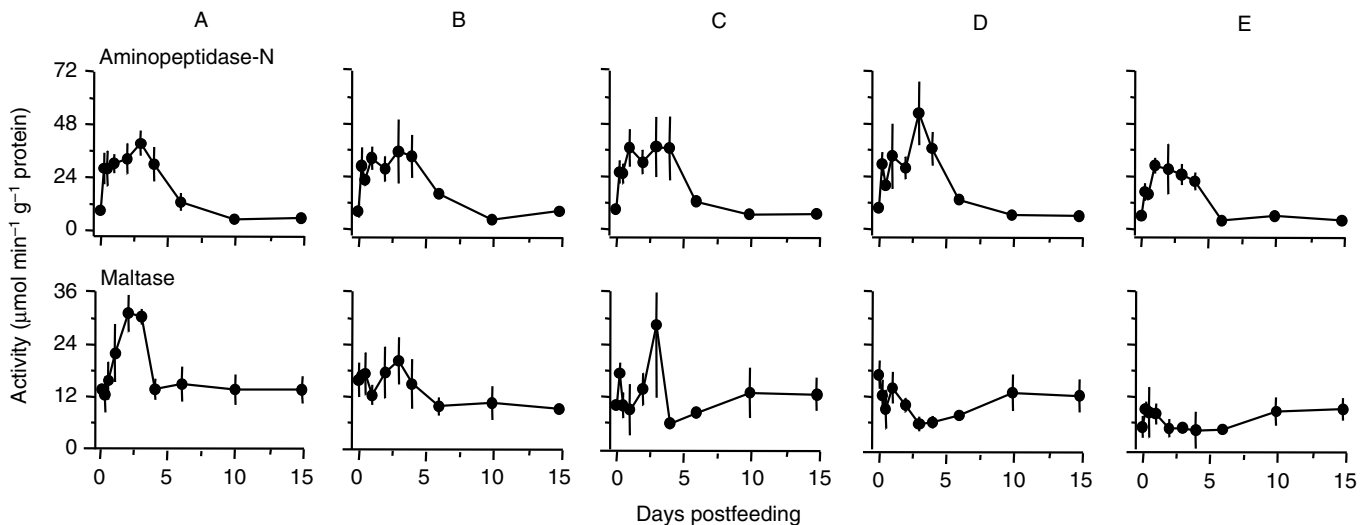


Fig. 6. Intestinal aminopeptidase-N and maltase activity of each intestinal segment (A, B, C, D and E) of *Python molurus*. Note the postprandial increase in hydrolase activity for much of the python's small intestine.

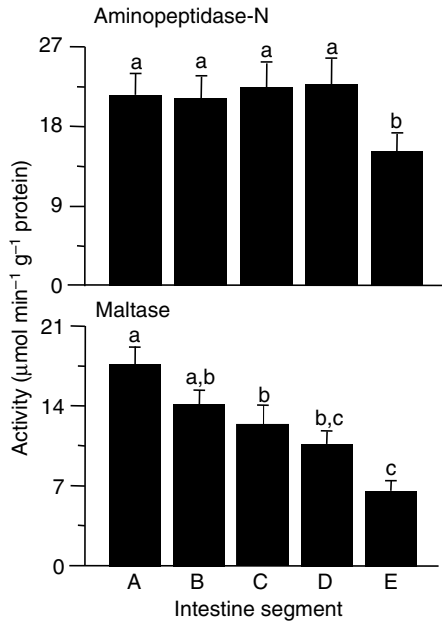


Fig. 7. Aminopeptidase-N (APN) and maltase activity averaged over all sampling periods for each intestinal segment (A, B, C, D and E) of *Python molurus*. Note the decline distally in activity for both hydrolases. In this and the following bar graphs, error bars indicate ± 1 s.e.m. and different letters above the bars denote significant ($P < 0.05$) differences between means as determined from *post-hoc* pairwise comparisons.

DISCUSSION

Burmese pythons exhibit concomitant postprandial increases in gastrointestinal organ mass, digestive enzyme action, and nutrient transport. Moreover, the temporal profile of these trophic and functional responses are remarkably similar, peaking between 1 and 4 days after feeding and returning to fasted levels, usually by 10 days following feeding. In the ensuing discussion we will address patterns and mechanisms of gastrointestinal morphological and performance upregulation, as well as elaborate on the coordinated response of the python digestive tract to feeding.

Tissue responses to feeding

We found the pancreas and small intestine, but not the stomach, to increase in mass after feeding. Similar studies have documented pancreatic hypertrophy with feeding for the anurans *Ceratophrys ornatus* and *Pyxicephalus adspersus*, as well as the snakes *Boa constrictor* and *Python brongersmai* (Secor and Diamond, 2000; Secor, 2005a; Ott and Secor, 2007). The postprandial increase in pancreas mass may result from hypertrophy of acinar and ductal cells in response to the respective increased demand for the production and secretion of digestive enzymes and the buffering sodium bicarbonate. For all five segments of the small intestine there was a significant postprandial increase in the mass of the mucosa, whereas the muscularis/serosa component did not change in mass with feeding. For Burmese pythons, feeding triggers a 40% increase in the volume of the intestinal enterocytes, which results in a lengthening of the intestinal villi (Lignot et al., 2005). Once digestion has been completed, the python intestine undergoes atrophy, marked by a reduction in enterocyte volume and mucosal mass. Fasting-induced atrophy of the small intestine mucosa and rapid hypertrophy with refeeding is a well-documented physiological phenomenon, having been observed for fish, amphibians, reptiles,

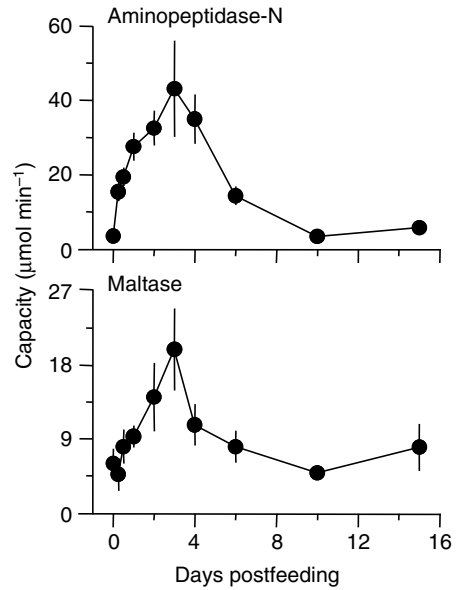


Fig. 8. Intestinal aminopeptidase-N (APN) and maltase capacity as a function of days postfeeding for *Python molurus*. Both intestinal APN and maltase capacity increase rapidly after feeding before returning to values by day 10.

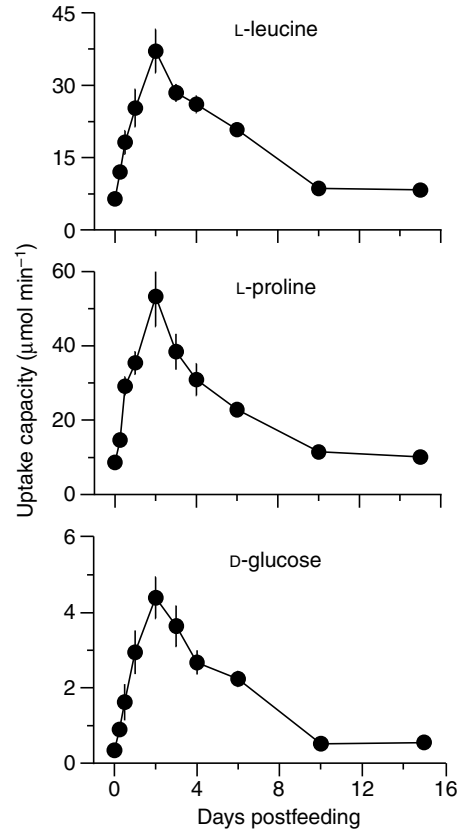


Fig. 9. Intestinal L-leucine, L-proline and D-glucose uptake capacities as a function of days postfeeding for *Python molurus*. Note that the y-axis scales are different for the three different nutrient transporters. Pythons experience significant postprandial increases in uptake capacities for the three nutrients.

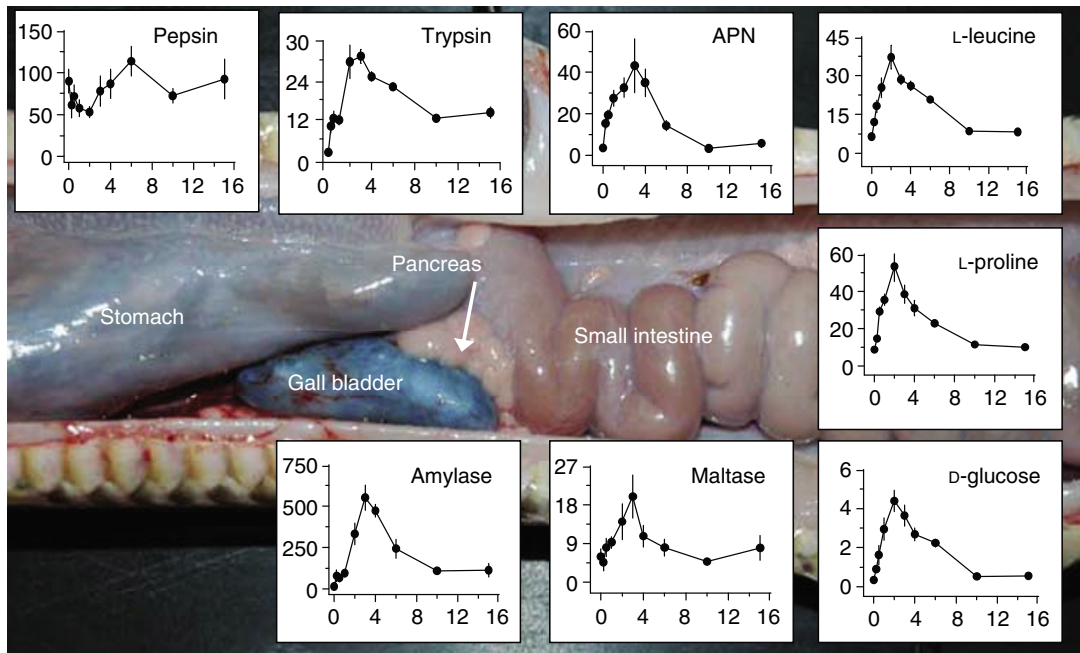


Fig. 10. Capacities of enzyme activities and nutrient transport in *Python molurus*. Each graph (previously presented in Figs 4, 5, 8 and 9) represents the capacity of enzyme activity or nutrient activity ($\mu\text{mol min}^{-1}$) as a function of days postfeeding. Graphs are located above and below the organ from which the respective enzymes originate. Note the synchronous regulatory response of components of both protein and carbohydrate digestion and absorption for these pythons.

birds and mammals (Carey, 1990; Hall and Bellwood, 1995; Karasov et al., 2004; Secor, 2005a; Ott and Secor, 2007).

Gastric function

The first indication of an increase in gastric function occurred 12 h after feeding when 1.5% of the ingested meal had passed into the small intestine. At this time, stomach pH had dropped from a fasting level of 6.5 to 2, and the food items showed signs of digestion as the skull of the rats were partially exposed (Secor et al., 2006). Over the next 12 h, an additional 15.5% of the ingested meal had been passed from the stomach, at an average clearance rate of 1.25 g h^{-1} (Fig. 3). By day 3, 26% of the ingested meal remained in the stomach, largely composed of some teeth, disarticulated bones, and hair. By day 6, the only remnant of the meal within in the stomach was a mat of hair. Our analysis of pepsin activity of the gastric mucosa correlated well in time with meal breakdown. Pepsin activity was highest in fasted snakes and following the completion of digestion, and lowest during gastric breakdown. Remember, in our assay we generated pepsin from the inactive precursor pepsinogen, which is produced and stored within zymogen granules within oxyntopeptic cells. Hence, high pepsin activity is indicative of large amounts of stored pepsinogen, whereas low pepsin activity suggests the prior release of pepsinogen. We found oxyntopeptic cells of fasted pythons to possess numerous zymogen granules, whereas few granules were observed after feeding (Fig. 11). Pythons store pepsinogen during fasts in order to immediately release it with feeding. In similar fashion, tissue concentration of gastrointestinal hormones are highest in fasted pythons and lowest after feeding, corresponding to a rapid postprandial increase in plasma concentration of these hormones (Secor et al., 2001). In contrast to our results, feeding induced a 7.5-fold increase in stomach pepsin activity in the snake, *Natrix tessellata* (Zalkah and Bdolah, 1987).

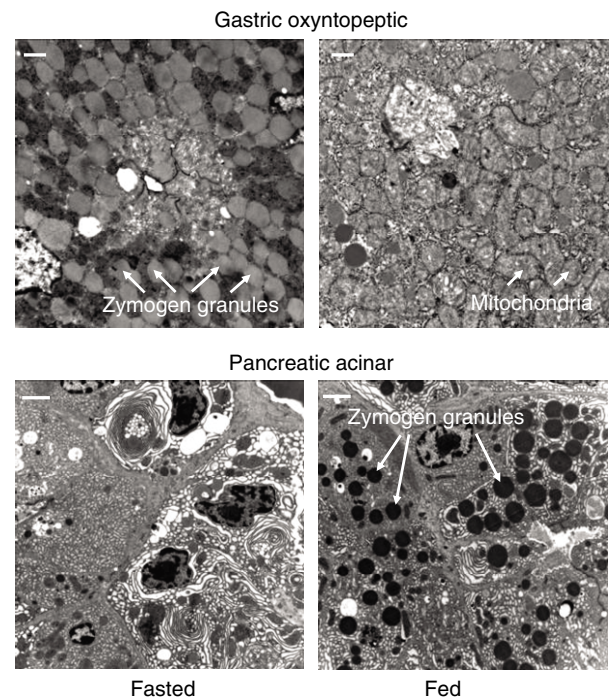


Fig. 11. Transmission electron micrographs of gastric oxyntopeptic and pancreatic acinar cells of fasted (left) and fed (right) *Python molurus*. Note the numerous zymogen granules containing inactive enzymes within the oxyntopeptic cells of fasted pythons and within the acinar cells of fed pythons. By contrast, oxyntopeptic cells of fed snakes and acinar cells of fasted snakes possessed few zymogen granules. Scale bars, $1 \mu\text{m}$.

Regulation of pancreatic enzymes

The postfeeding regulation of amylase and trypsin activity followed similar patterns, both peaking at day 4 and returning to prefeeding levels by day 10. The upregulation of these enzymes with feeding reflects the increased demand to hydrolyze meal proteins and carbohydrates. Hence the greatest increase in small intestine contents occurs between 12 and 24 h after feeding, coinciding with significant increases in amylase and trypsin activity. The increase in the production of pancreatic enzymes is triggered by cholecystokinin (CCK), an intestinal hormone secreted when food enters the small intestine (Kutchai, 2004). Plasma concentrations of CCK are upregulated within 6 h after feeding and peak at day 1 of digestion in the Burmese python (Secor et al., 2001). Postprandial increases in volume and enzyme activity of pancreatic secretions have been documented for dogs (Shylgin and Vasilevskya, 1974). Similarly, in the snake, *Natrix tessellata*, feeding induces a respective 190% and 200% increase in the activity of chymotrypsin (peptidase) and amylase (Zalkah and Bdollah, 1987). Trypsin resides in the pancreas as inactive trypsinogen, and becomes activated to trypsin during the assay. Hence, it is uncertain the extent that trypsinogen is released and activated within the python's intestinal lumen after feeding. By assaying intestinal luminal contents, we observed a postprandial increase in the presence of active trypsin within the intestine. Whereas the stomach data suggest the storage of pepsinogen during periods of fasting, the low levels of amylase and trypsinogen within the pancreas during fasting indicates that these enzymes are instead synthesized immediately after feeding. Preliminary observations of pancreatic histology reveal the absence of enzyme-containing zymogen granules within acinar cells of fasted pythons and their presence within these cells of digesting snakes (Fig. 11).

Temporal variation in intestinal function

For all five indices of intestinal performance (capacities of two hydrolases and three nutrient transporters), we observed matched upregulation that peaked at 2 or 3 days postfeeding, and subsequently declined to fasting levels by day 10 (Figs 8 and 9). The response to feeding and fasting of intestinal hydrolases and nutrient transporters are mixed among vertebrates. Hibernation-induced fasting results in increased activity of intestinal hydrolases and nutrient transport among rodents (Galluser et al., 1998; Carey and Sills, 1992). Feeding was found not to elicit any changes in APN or maltase activity for the cedar waxwing (*Bombycilla cedrorum*) or Andean toad (*Bufo spinulosus*), and no change in intestinal nutrient uptake rates for frequently feeding anurans and snakes (McWilliams et al., 1999; Secor and Diamond, 2000; Naya et al., 2004; Secor, 2005b). By contrast, intestinal hydrolase and transporter activities are upregulated after feeding in estivating anurans, the binge-feeding Gila monster *Heloderma suspectum*, and infrequently feeding snakes (Secor, 2005b; Christel et al., 2007; Ott and Secor, 2007).

In comparing the separate pathways of intestinal digestion and absorption of protein and carbohydrates, the scope of response for the carbohydrates (3- to 12-fold) was similar to the scope of response for proteins (6- to 12-fold). However, with the exception of pancreatic amylase, measured magnitude of activity was considerably greater for the protein pathway, as intestinal amino acid uptake rates and APN activity were up to ten times that of intestinal D-glucose uptake and maltase activity. We acknowledge that the differences in amino acid *versus* glucose uptake may in part be explained by our methods, which measured both active and passive uptake of the amino acids and only active uptake of D-glucose. Regardless, the difference in protein and carbohydrate digestion reflects the adaptive matching of meal composition and

intestinal performance. As strict carnivores, the python's diet is high in protein and low in carbohydrates (estimated to be 60% and 5% of dry mass, respectively); and hence the emphasis on protein digestion and amino acid absorption. In fact, we did not detect the presence of either lactase or sucrase in the python's small intestine using a similar assay as that for maltase (Dahlqvist, 1984).

There are three proposed mechanisms whereby mass specific rates of enzyme and transporter activities can be modulated after feeding (Ferraris, 1994). The first is a change in the specific activity of enzymes and/or transporters (due to cellular activation or deactivation). Second is a change in the membrane density of enzymes and transporters, brought on by an increase or decrease of synthesis and/or translocation from the cytoplasm to the cell membrane. The third mechanism involves an alteration in functional surface area while maintaining protein density and activity, hence any change in the amount of luminal surface area will impact intestinal performance. Whereas the first two mechanisms have been implicated in shifts of digestive function for mammals (Buddington and Diamond, 1989; Ferraris et al., 1992), it is the third mechanism that appears to largely contribute to the regulation of intestinal function in pythons (Secor, 2005b). The evidence for such a structural mechanism in pythons is the rapid fourfold postprandial increase in intestinal microvillus length and the subsequent decrease in length once digestion has been completed (Lignot et al., 2005). This plasticity of microvillus surface area matches closely with the observed postprandial modulation of enzyme and transporter activities. If the magnitude of increase in function exceeds that explained by the change in surface area, then one or both of the other mechanisms is likely contributing to the upregulatory response.

A proximal to distal gradient of intestinal morphology and function has been noted for fishes, amphibians, reptiles, birds and mammals (Karasov et al., 1983; Secor and Diamond, 2000; Witmer and Martinez del Rio, 2001; Kroghdahl and Bakke-Mckellep, 2005; Secor, 2005a). For the Burmese python, evidence of these gradients include a 37%, 51% and 39% decline, respectively, in the wet mass, APN activity and maltase activity for segment E compared with segment A. A mechanistic explanation for the distal decline in function is a reduction in the intestinal epithelium, shorter microvilli, an increase in the population of goblet cells, and a corresponding decrease in enterocyte density (Lignot et al., 2005). An adaptive explanation reflects the decline distally in demand as the concentration of luminal nutrients is reduced. The much higher concentration of proteins in their diet compared to carbohydrate may explain why APN activity does not decline over much of the length of the small intestine, whereas maltase activity begins to decline almost immediately (Fig. 6).

Integrated response

Digestion is a coordinated, integrative process involving the interactions of hormones, smooth muscle contractions, gastric, biliary and pancreatic secretions, and epithelial hydrolases and transporters. For the Burmese python, we found remarkable similarities in the postprandial pattern and timing of gastric, pancreatic and intestinal performance (Fig. 10). These snakes experience increases in GI tissue mass and mass-specific rates of tissue function with feeding, combining to produce dramatic, and in some cases matched, upregulation of organ performance capacity. The striking concordance among intestinal morphology, enzyme activity and nutrient uptake indicate that all components of Burmese python digestion must be upregulated for digestion to match dietary load.

In the python, the sequence of the integrated response to feeding begins with the swallowing of prey, whereupon the release of neurotransmitters and hormones (i.e. acetylcholine and gastrin) trigger the production of gastric acid and the release of pepsinogen. The lowering of stomach luminal pH to 1 and the conversion of pepsinogen to pepsin results in the breakdown of the intact meal (including bones) to a soup-like chyme (Secor, 2003). Entry of this chyme (7.4 ± 0.9 g within the first 24 h of this study) into the small intestine induces the release of a host of GI regulatory peptides, including CCK, glucose-dependent insulinotropic peptide and neurotensin (Secor et al., 2000b; Secor et al., 2001). These specific peptides and others (e.g. secretin) may in part stimulate gall bladder contraction and the 3- to 30-fold increases in pancreatic and intestinal performance. The postprandial release of bile into the small intestine is indicated by the 64% decline in gall bladder mass (Secor and Diamond, 1995). The pancreas responds by doubling its mass and increasing the production and release of enzymes and sodium bicarbonate, the latter indicated by the rapid increase (within 5 cm of the pylorus) in luminal pH (to 6) of the proximal small intestine (Secor et al., 2006). Pancreatic enzymes reduce luminal proteins and carbohydrates to oligopeptides and disaccharides, respectively, which then face the upregulated membrane-bound oligopeptidases (e.g. aminopeptidase-N) and the disaccharidase maltase. Once cleaved, amino acids and glucose are readily transported across the brushborder membrane and into circulation, facilitated by the combined increases in mucosal mass, mass-specific nutrient uptake rates and intestinal blood flow (Secor, 2005b). As quickly as the python's gastrointestinal system upregulates form and function with feeding, it downregulates performance at an apparently similar pace following the emptying of the stomach and small intestine. By day 10 postfeeding, stomach pH had returned to 6.5, pepsinogen remains within the gastric epithelium, pancreatic enzymes have declined in activity, and the activities of intestinal hydrolases and transporters have returned to their fasting levels.

Coordination of morphology and capacity with functional load in physiological systems was first examined in the mammalian pulmonary system, and was termed symmorphosis (Taylor and Weibel, 1981). Pulmonary ventilation and diffusion, circulatory convection, skeletal muscle diffusion, and mitochondrial oxidative phosphorylation were measured for African mammals (Taylor and Weibel, 1981), dogs, ponies, calves and goats (Weibel et al., 1987), and within the network of oxidative pathways in dogs and goats (Taylor et al., 1996). These studies revealed that for most components of the mammalian pulmonary system there is a matched response to changes in demand. Our results agree with the general prediction of symmorphosis, namely that there is coordinated regulation of each component of the Burmese python's GI tract in response to the demand of digestion and absorption. Presumably, any tissue of the python's GI tract that does not upregulate performance with feeding would generate a bottleneck, thereby limiting the rate of digestion and resulting in an inefficiency of energy and space (Diamond, 2002). Similarly, any tissue that does not downregulate performance with fasting would theoretically also represent an unnecessary loss of energy.

Further research

This research, in demonstrating matched responses of morphology, enzyme activity and nutrient uptake in the Burmese python has revealed a pair of interesting questions that deserve further attention. First, whereas we have described the regulation of both carbohydrate and protein digestion, equally important for carnivores is the digestion and absorption of lipids. Within the small intestine, lipids

are broken down *via* the combined actions of gastric and pancreatic lipases and biliary secretions and then passively absorbed into the enterocytes (Starck and Beese, 2001; Lignot et al., 2005). For Burmese pythons, it has already been noted that gall bladder contents decrease 64% with feeding, indicating the postprandial release of bile (Secor and Diamond, 1995). Unknown is the extent that the activity of pancreatic lipase is regulated with feeding in the python and whether the magnitude of regulation varies with meal fat content.

Second, species of snakes that feed relatively frequently experience modest regulation of intestinal nutrient uptake with feeding and fasting (Secor and Diamond, 2000). Hence it would be predicted that the activities of pancreatic and intestinal enzymes will also be modestly regulated through a feeding cycle for such snakes. Evidence of such a correlated response is the combined lack of significant postfeeding increases in intestinal amino acid uptake and APN activity in the Amazon tree boa *Corallus hortulanus*, a boid that feeds relatively frequently (Secor and Ott, 2007). Conducting similar experiments to those in this paper with snake species [e.g. *Coluber*, *Masticophis*, *Nerodia* and *Thamnophis* (Secor, 2005b)] that do not significantly regulate intestinal nutrient uptake capacity would further elucidate (at least for snakes) the adaptive match in regulation and performance of the various components of the digestive system.

We would like to extend our sincere appreciation to S. Boback, L. Kirby, B. Ott and J. Wooten for helpful comments on previous versions of this manuscript. We thank M. Addington, J. Barkley, S. Boback, A. Brooks, S. Cover, A. Deller, G. Gladden, L. Hays, S. Horace, E. Johnson, T. Jones, L. Medaris, E. Newsom, B. Nye, B. Ott and K. Picard for technical assistance during this project. Our sincere appreciation is extended to D. German for the pepsin activity protocol. This work was supported by the National Science Foundation (IOS-0466139 to S. Secor) and the University of Alabama.

REFERENCES

- Anson, M. L. (1938). The estimation of pepsin, trypsin, papain, and cathepsin with hemoglobin. *J. Gen. Physiol.* **22**, 79-89.
- Beall, C. M. (2006). Andean, Tibetan, and Ethiopian patterns of adaptation to high-altitude hypoxia. *Integr. Comp. Biol.* **46**, 18-24.
- Bernfeld, P. (1955). Amylases α and β . *Meth. Enzymol.* **1**, 149-158.
- Bradford, M. (1976). A rapid and sensitive method for the quantitation of microgram quantities of protein utilizing the principal of protein-dye binding. *Anal. Biochem.* **72**, 248-254.
- Buddington, R. K. and Diamond, J. M. (1989). Ontogenetic development of intestinal nutrient transporters. *Annu. Rev. Physiol.* **51**, 601-617.
- Carey, H. V. (1990). Seasonal changes in mucosal structure and function in ground squirrel intestine. *Am. J. Physiol.* **259**, R385-R392.
- Carey, H. V. and Sills, N. S. (1992). Maintenance of intestinal nutrient transport during hibernation. *Am. J. Physiol.* **263**, R517-R523.
- Christel, C. M., DeNardo, D. F. and Secor, S. M. (2007). Metabolic and digestive responses to food ingestion in a binge-feeding lizard, the Gila monster (*Heloderma suspectum*). *J. Exp. Biol.* **210**, 3430-3439.
- Cramp, R. L. and Franklin, C. E. (2005). Arousal and re-feeding rapidly restores digestive tract morphology following aestivation in green-striped burrowing frogs. *Comp. Biochem. Physiol.* **142A**, 451-460.
- Dahlqvist, A. (1984). Assay for intestinal disaccharidases. *Scand. J. Clin. Lab. Invest.* **44**, 69-172.
- Diamond, J. (2002). Quantitative evolutionary design. *J. Physiol.* **542**, 337-345.
- Dudley, R. and Gans, C. (1991). A critique of symmorphosis and optimality models in physiology. *Physiol. Zool.* **64**, 627-637.
- Ferraris, R. P. (1994). Regulation of intestinal nutrient transport. In *Physiology of the Gastrointestinal Tract* (ed. L. R. Johnson), pp. 1821-1844. New York: Raven Press.
- Ferraris, R. P., Villenas, S. A., Hirayama, B. A. and Diamond, J. (1992). Effect of diet on glucose transporter site density along the intestinal crypt-villus axis. *Am. J. Physiol.* **262**, G1060-G1068.
- Fudge, D. S., Ballantyne, J. S. and Stevens, E. D. (2001). A test of biochemical symmorphosis in a heterothermic tissue: bluefin tuna white muscle. *Am. J. Physiol.* **280**, R108-R114.
- Galluser, M., Raul, F. and Canguilhem, B. (1988). Adaptation of intestinal enzymes to seasonal and dietary changes in a hibernator: the European hamster (*Cricetus cricetus*). *J. Comp. Physiol. B* **158**, 143-149.
- Garland, T. R. and Huey, R. B. (1987). Testing symmorphosis: does structure match functional requirements? *Evolution* **41**, 1404-1409.
- Habold, C., Chevalier, C., Dunel-Erb, S., Foltzer-Jourdainne, C., Maho, Y. L. and Lignot, J. H. (2004). Effects of fasting and refeeding on jejunal morphology and cellular activity in rats in relation to depletion of body stores. *Scand. J. Gastroenterol.* **39**, 531-539.
- Hall, K. C. and Bellwood, D. R. (1995). Histological effects of cyanide, stress and starvation on the intestinal mucosa of *Pomacentrus coelestis*, a marine aquarium fish species. *J. Fish Biol.* **47**, 438-454.

- Hammond, K. A. and Diamond, J.** (1994). Limits to nutrient intake and intestinal nutrient uptake capacity during extended lactation. *Physiol. Zool.* **67**, 282-303.
- Karasov, W. H. and Diamond, J.** (1983). A simple method for measuring intestinal solute uptake *in vitro*. *J. Comp. Physiol. B* **152**, 105-116.
- Karasov, W. H., Pond, R. S., Solberg, D. H. and Diamond, J. M.** (1983). Regulation of proline and glucose transport in mouse intestine by dietary substrate levels. *Proc. Natl. Acad. Sci. USA* **80**, 7674-7677.
- Karasov, W. H., Pinshow, B., Starck, J. M. and Afik, D.** (2004). Anatomical and histological changes in the alimentary tract of migrating blackcaps (*Sylvia atricapilla*): a comparison among fed, fasted, food-restricted, and refed birds. *Physiol. Biochem. Zool.* **77**, 149-160.
- Krogdahl, Å. and Bakke-Mckellep, A. M.** (2005). Fasting and refeeding cause rapid changes in intestinal tissue mass and digestive enzyme capacities in Atlantic salmon (*Salmo salar* L.). *Comp. Biochem. Physiol.* **141A**, 450-460.
- Kutchai, H. C.** (2004). The gastrointestinal system. In *Physiology* (5th edn) (ed. R. M. Berne, M. N. Levy, B. M. Koepfen and B. A. Stanton), pp. 567-620. St Louis, MO: Elsevier Press.
- Lam, M. M., O'Connor, T. P. and Diamond, J.** (2002). Loads, capacities, and safety factors of maltase and the glucose transporter SGLT1 in mouse intestinal brush border. *J. Physiol.* **542**, 493-500.
- Lignot, J. H., Helmstetter, C. and Secor, S. M.** (2005). Postprandial morphological response of the intestinal epithelium of the Burmese python (*Python molurus*). *Comp. Biochem. Physiol.* **141A**, 280-291.
- Lindstedt, S. L. and Jones, J. H.** (1988). Symmorphosis: the concept of optimal design. In *New Directions in Ecological Physiology* (ed. M. E. Feder, A. F. Bennett, W. W. Burggren and R. B. Huey), pp. 109-289. Cambridge: Cambridge University Press.
- McDonagh, M. J. N. and Davies, C. T. M.** (1984). Adaptive response of mammalian skeletal muscle to exercise with high loads. *Eur. J. Appl. Physiol.* **52**, 139-155.
- McWilliams, S. R. and Karasov, W. H.** (2001). Phenotypic flexibility in digestive system structure and function in migratory birds and its ecological significance. *Comp. Biochem. Physiol.* **128A**, 579-593.
- McWilliams, S. R., Caviedes-Vidal, E. and Karasov, W. H.** (1999). Digestive adjustments in cedar waxwings to high feeding rate. *J. Exp. Zool.* **283**, 394-407.
- Naya, D. E., Farfan, G., Sabat, P., Mendez, M. E. and Bozinovic, F.** (2004). Digestive morphology and enzyme activity in the Andean toad *Bufo spinulosus*: hard-wired or flexible physiology? *Comp. Biochem. Physiol.* **140A**, 165-170.
- O'Connor, T. P. and Diamond, J. M.** (1999). Ontogeny of intestinal safety factors: lactase capacities and lactase loads. *Am. J. Physiol.* **276**, R753-R765.
- Ott, B. D. and Secor, S. M.** (2007). Adaptive regulation of digestive performance in the genus *Python*. *J. Exp. Biol.* **210**, 340-356.
- Overgaard, J., Busk, M., Hicks, J. W., Jensen, F. B. and Wang, T.** (1999). Respiratory consequences of feeding in the snake *Python molurus*. *Comp. Biochem. Physiol.* **205A**, 3327-3334.
- Overgaard, J., Andersen, J. B. and Wang, T.** (2002). The effects of fasting duration on the metabolic response to feeding in *Python molurus*: an evaluation of the energetic costs associated with gastrointestinal growth and upregulation. *Physiol. Biochem. Zool.* **75**, 360-368.
- Piersma, T. and Lindström, Å.** (1997). Rapid reversible changes in organ size as a component of adaptive behaviour. *Trends Ecol. Evol.* **12**, 134-138.
- Preiser, H., Schmitz, J., Maestracci, D. and Crane, R. K.** (1975). Modification of an assay for trypsin and its application for the estimation of enteropeptidase. *Clin. Chim. Acta* **59**, 169-175.
- Salvador, A. and Savageau, M. A.** (2003). Quantitative evolutionary design of glucose-6-phosphate dehydrogenase expression in human erythrocytes. *Proc. Natl. Acad. Sci. USA* **100**, 14463-14468.
- Shylgin, G. K. and Vasilevska, L. S.** (1974). Enzyme secreting processes in the pancreas during starvation. *Bull. Exp. Biol.* **77**, 27-30.
- Secor, S. M.** (2003). Gastric function and its contribution to the postprandial metabolic response of the Burmese python *Python molurus*. *J. Exp. Biol.* **206**, 1621-1630.
- Secor, S. M.** (2005a). Physiological responses to feeding, fasting, and estivation for anurans. *J. Exp. Biol.* **208**, 2595-2608.
- Secor, S. M.** (2005b). Evolutionary and cellular mechanisms regulating intestinal performance of amphibians and reptiles. *Integr. Comp. Biol.* **45**, 66-78.
- Secor, S. M. and Diamond, J.** (1995). Adaptive responses to feeding in Burmese pythons: pay before pumping. *J. Exp. Biol.* **198**, 1313-1325.
- Secor, S. M. and Diamond, J.** (1997). Determinants of the postfeeding metabolic response in Burmese pythons (*Python molurus*). *Physiol. Zool.* **70**, 202-212.
- Secor, S. M. and Diamond, J.** (1998). A vertebrate model of extreme physiological regulation. *Nature* **395**, 659-662.
- Secor, S. M. and Diamond, J.** (2000). Evolution of regulatory responses to feeding in snakes. *Physiol. Biochem. Zool.* **73**, 123-141.
- Secor, S. M. and Ott, B. D.** (2007). Adaptive correlation between feeding habits and digestive physiology for boas and pythons. In *Biology of the Boas and Pythons* (ed. R. W. Henderson and R. Powell), pp. 257-268. Eagle Mountain, UT: Eagle Mountain Publishing.
- Secor, S. M., Stein, E. D. and Diamond, J.** (1994). Rapid upregulation of snake intestine in response to feeding: a new model of intestinal adaptation. *Am. J. Physiol.* **266**, G695-G705.
- Secor, S. M., Hicks, J. W. and Bennet, A. F.** (2000a). Ventilatory and cardiovascular responses of a python (*Python molurus*) to exercise and digestion. *J. Exp. Biol.* **203**, 2447-2454.
- Secor, S. M., Whang, E. E., Lane, J. S., Ashley, S. W. and Diamond, J.** (2000b). Luminal and systemic signals trigger intestinal adaptation in the juvenile python. *Am. J. Physiol.* **279**, G1177-G1187.
- Secor, S. M., Fehsenfeld, D., Diamond, J. and Adrian, T. E.** (2001). Responses of python gastrointestinal regulatory peptides to feeding. *Proc. Natl. Acad. Sci. USA* **98**, 13637-13642.
- Secor, S. M., Boback, S. M. and Lignot, J.-H.** (2006). Spatial and temporal variation in the pH of the gastrointestinal tract of the Burmese python. *Integr. Comp. Biol.* **46**, e128.
- Starck, J. M. and Beese, K.** (2001). Structural flexibility of the intestine of Burmese python in response to feeding. *J. Exp. Biol.* **204**, 325-335.
- Taylor, C. R. and Weibel, E. R.** (1981). Design of the mammalian respiratory system. I. Problem and strategy. *Respir. Physiol.* **44**, 1-10.
- Taylor, C. R., Weibel, E. R., Weber, J. M., Vock, R., Hoppeler, H., Roberts, T. J. and Brichton, G.** (1996). Design of the oxygen and substrate pathways. I. Model and strategy to test symmorphosis in a network structure. *J. Exp. Biol.* **199**, 1643-1649.
- Weibel, E. R., Taylor, C. R., Hoppeler, H. and Karas, R. H.** (1987). Adaptive variation in the mammalian respiratory system in relation to energetic demand. I. Introduction to problem and strategy. *Respir. Physiol.* **69**, 1-127.
- Weibel, E. R., Taylor, C. R. and Hoppeler, H.** (1991). The concept of symmorphosis, a testable hypothesis of structure-function relationship. *Proc. Natl. Acad. Sci. USA* **88**, 10357-10361.
- Weiss, S. L., Lee, E. A. and Diamond, J.** (1998). Evolutionary matches of enzyme and transporter capacities to dietary substrate loads in the intestinal brush border. *Proc. Natl. Acad. Sci. USA* **95**, 2117-2121.
- Witmer, M. C. and Martinez del Rio, C.** (2001). The membrane-bound intestinal enzymes of waxwings and thrushes: adaptive and functional implication of patterns of enzyme activity. *Physiol. Biochem. Zool.* **74**, 584-593.
- Wojnarowska, F. and Gray, G. M.** (1975). Intestinal surface peptide hydrolases: identification and characterization of three enzymes from rat brush border. *Biochem. Biophys. Acta* **403**, 147-160.
- Zalkah, M. and Bdolah, A.** (1987). Dietary regulation of digestive enzyme levels in the water snake, *Natrix tessellata*. *J. Exp. Zool.* **243**, 9-13.